SSC19-III-08

CubeSat Laser Communication Crosslink Pointing Demonstration

Richard P. Welle, Christopher M. Coffman, Dee W. Pack, and John R. Santiago
The Aerospace Corporation
PO Box 92957
Los Angeles, CA, USA, 90009
welle@aero.org

ABSTRACT

An opportunity arose to demonstrate optical crosslink pointing between two CubeSats in LEO using spacecraft not specifically designed for that purpose. The AeroCube-7 spacecraft, designed for optical downlinks as part of the Optical Communication and Sensor Demonstration mission, was tasked to point its communications laser at the ISARA spacecraft to demonstrate the capability of one CubeSat to track another in LEO. The ISARA spacecraft, which does not carry a data receiver, but does carry a short-wave infrared camera (SWIR) as part of the CUMULOS payload, was tasked to track the AeroCube-7 spacecraft and use the SWIR camera to record the OCSD laser. The SWIR images were downloaded over an RF channel and used to evaluate the pointing and tracking of both spacecraft. Two successful tests of crosslink pointing were completed between AeroCube-7 and ISARA, providing a demonstration in principle of the capability, and laying the groundwork for more refined experiments that will use this technique for on-orbit measurements of beam profiling. Further tests between AeroCube-11 and ISARA are also in preparation to demonstrate crosslink pointing in a more-challenging orbital configuration.

INTRODUCTION

A common challenge in developing small-satellite-based Earth-observation (EO) missions is getting the data to the ground. For many next-generation EO missions, such as hyperspectral imaging or SAR missions, the volume of data generated is large enough to tax most conventional radio-frequency (RF) downlink systems. For other EO missions, such as hazard monitoring or data collection for weather forecasting, data latency is a key issue. It is well known that laser downlinks offer the potential of multi-gigabit-per-second download speeds, which are typically two to three orders of magnitude faster than RF downlink speeds. On the other hand, optical downlink systems can easily be interrupted at any given ground station (possibly for long periods) due to cloud cover.

An approach that could support high-volume and low-latency communication requirements is to develop a network of small optical relay satellites in LEO that provide a communications service throughout LEO space by receiving EO data and relaying it around the Earth to a satellite in view of an optical ground station not obscured by clouds. While any individual ground station may be obscured by clouds at any time, ground stations placed in locations selected for good seeing conditions will, on average, be accessible well more than 50 % of the time. If enough ground stations are placed in locations separated geographically by distances large enough that there is little to no correlation in weather between stations, then the probability of there being at least one ground station available can be near unity.

Beyond the deployment of sufficient ground stations, such a system requires the development of both small-satellite optical downlinks and small-satellite optical crosslinks. The first CubeSat-based optical downlink was demonstrated last year using two 1.5U satellites developed under the NASA Optical Communication and Sensor Demonstration (OCSD) program. These satellites, AeroCube-7 B & C, carried laser transmitters for the downlink demonstration, but not laser receivers as would be required for a full crosslink communication demonstration. However, beyond the laser transmitter, the principal challenge for laser communication is the precise pointing required to get the laser beam to the intended receiver, and it is possible to demonstrate pointing capability without having a high-speed receiver if the beam signal strength can be measured at the target. The OCSD program demonstrated the ability of the satellites to point at a stationary ground target in the downlink demonstration, but tracking a moving target in space for a crosslink presents a different challenge. In principle, all motion is relative, and the ground station is moving with respect to an Earth-centered inertial frame of reference. However, the ground station is at a known location on the Earth's surface, and the motion of the Earth's surface with respect to the inertial frame is very well characterized allowing the position of the ground station to be forecast with a high degree of accuracy for any time

period that may be of interest to a communications program.

The same cannot be said of satellites in orbit. Satellite motion is defined primarily by the local gravitational field. However, various non-gravitational forces also act on satellites in orbit, and of these forces atmospheric drag in particular becomes much more significant as the orbital altitude decreases (more atmosphere), and as the satellite size decreases (higher drag per unit mass). Natural variations in the density of the upper atmosphere, driven primarily by variations in solar activity, are not generally predictable on a time scale relevant to orbital dynamics, so forecasts of the location of small satellites in LEO will necessarily come with some uncertainty. The degree of uncertainty depends on the approach used for orbit determination. In LEO CubeSats, orbit determination is often based on GPS readings, and the position uncertainty can typically be reduced to the range of a few meters on a short (of order one day) forecast.

For an optical transmission from a LEO satellite, the required pointing vector, which continuously changes with time, is determined by the location of both the transmitter and the intended receiver. For the downlink case, the location of the receiver is well known (although atmospheric effects can affect beam quality, and even pointing requirements for ultra-narrow beams). In addition, in the downlink case, the motion of the transmitter relative to the receiver is limited by orbital dynamics and the minimum orbital altitude such that the slew rate of the transmitter never has to exceed about 1 degree per second. For the crosslink case, the locations of both the transmitter and the receiver are uncertain, and relative motion is not similarly constrained.

Two approaches are commonly used to deal with location uncertainty. In closed-loop pointing, a beacon is directed toward the sender by the receiver to provide real-time tracking information to the sender. Uncertainties in location of the sender and receiver are significant only if they are large enough that they could impact the ability of the beacon to hit a detector on the transmitter satellite, and this issue can be resolved by making the beacon beamwidth sufficiently large. With the location uncertainty resolved by the beacon, the communications beam divergence need only be wide enough to cover uncertainties in the pointing accuracy of the sender, without regard to orbit-determination uncertainties. In open-loop pointing, the pointing vector is calculated based on the best-available information about the locations of the sender and receiver and the transmitted beam divergence is selected to be large enough to cover both the uncertainties in the pointing accuracy of the sender and the expected range of uncertainty in the locations of both the sender and the receiver. For small satellites, particularly CubeSats, the simplicity of not having to carry beacon transmitters and receivers suggests that open-loop pointing may be preferred if it can be operated reliably.

Ironically, for an open-loop tracking system using a fixed beam divergence, pointing and tracking will be easier for distant targets than for nearby targets for two reasons. First, with a fixed beam divergence, the spot size at the target will be smaller for nearby targets so any orbit ephemeris uncertainty becomes more significant. Consider, for example, a laser transmitter with a beam divergence of one milliradian. At a range of one thousand km, the spot diameter will be one km. If the positional uncertainties of the sender and receiver are each on the order of 10 m, the spot size will be much larger than any pointing errors associated with positional uncertainty. On the other hand, if the range is only 10 km, then the spot diameter at the target will be only 10 m, and the pointing errors associated with positional uncertainty may be large enough that the spot does not fall on the receiver. This effect becomes more significant as the beam divergence gets smaller. A second issue arises when the sender and receiver are passing close to one another, but not in the same orbit. In this case, the slew rate required for the sender to track the receiver can be very large and may exceed the slew-rate capabilities of the tracking system. As such, for these two reasons, any given transmitter will likely have a minimum operating distance for crosslinks.

One consequence of basing a relay network on small satellites is that there will be a practical upper limit to the size of the transmitter optics and, because of diffraction effects, a limit to how small the beam divergence can be. The minimum diffraction-limited beam divergence is proportional to the ratio of the laser wavelength to the diameter of the output optics. The proportionality constant is on the order of one, with the exact value depending on how beam divergence is defined. Some use the concept of Full-Width Half-Maximum (FWHM) to define beam divergence; i.e., the angle defined by two points in the far field on opposite sides of the beam where the intensity is half the peak intensity, with the apex of the angle at the beam source. Others use the $1/e^2$ radius; i.e., the angle between the beam centerline and a line from the beam source to a point in the far field where the beam intensity is $1/e^2$ (~0.135) times the peak intensity. Ultimately the practical beam divergence must be defined according to the margin built into the system; if the system can operate reliably with a received signal intensity of 1/2 the peak intensity, then the effective beam divergence is defined by the FWHM. If the system requires more than

half of the peak intensity to operate reliably, then the effective beam divergence will be smaller than the FWHM. In any case, it is not possible for the beam divergence to be smaller than approximately the ratio of the wavelength and the source diameter. Thus, for a system operating at a wavelength of 1550 nm with a 10-cm output optic (which is a reasonable upper limit for a CubeSat-based system), the diffraction-limited $1/e^2$ beam divergence will be about 5 microradians as measured by the beam radius or 10 microradians (about 0.57 millidegrees) when measured by the beam diameter. A beam pointing system for this transmitter would need to have an accuracy somewhat better than 5 microradians to ensure that the target is illuminated at an intensity above the $1/e^2$ limit, but there is no benefit in having a pointing system that is an order of magnitude more accurate than 5 microradians. Since beam divergence scales inversely with the diameter of the optics, smaller optical systems require correspondingly less accuracy of their pointing systems.

Similarly, the requirements for orbit determination are less stringent for small satellites (with diffraction-limited beam divergences) than for large satellites. A 10-microradian beam at a range of 1000 km will have a spot diameter of 10 m; if orbit position uncertainty is significantly smaller than that, then it will not have an impact on the beam pointing requirements.

Since beam pointing and tracking in crosslinks presents somewhat different challenges than in downlinks, we determined that it would be worthwhile to begin experiments on pointing even independent of the ability to actually receive high-speed communications data. An opportunity arose to test the crosslink tracking capability of the OCSD spacecraft by imaging the 1.064-nm lasers using the short-wave infrared (SWIR) camera that flew on the ISARA satellite as part of the CUMULOS payload. Although this camera is incapable of high-speed data reception, it is capable of acquiring images that can be used to estimate the laser beam intensity and confirm the tracking by OCSD of the ISARA spacecraft. A similar experiment will also be conducted using the laser transmitter on AeroCube-11, which is in an orbit that provides a somewhat more challenging tracking exercise.

EXPERIMENT

A total of four spacecraft, all CubeSats, were involved in various parts of this experimental effort. However, none of the four were designed with this experiment in mind; this was an experiment of opportunity using spacecraft capabilities designed for other purposes. The Optical Communication and Sensor Demonstration program supported the development and launch of two 1.5U CubeSats, AeroCube-7B and AeroCube-7C, also known as OCSD-B and OCSD-C, designed to demonstrate optical downlinks from LEO. These satellites each carry a single-stage Yb-fiber master-oscillator power-amplifier (MOPA) laser system designed to produce from 2 to 4 watts output at 1064 nm wavelength, and capable of being modulated at data rates of at least 200 Mb/s. The laser in OCSD-B has a fixed beam divergence of 0.06 degrees FWHM while the laser in OCSD-C has a fixed beam divergence of 0.15 degrees FWHM. The lasers are hard mounted to the satellite bodies and have no secondary beam steering system, so laser pointing is controlled entirely by controlling the spacecraft attitude. The spacecraft attitude-control system (ACS) includes a number of coarse attitude sensors (Earth nadir, Earth horizon, magnetometer, and sun sensors), a pair of custom-designed star cameras for fine attitude sensing, two three-axis rate gyros, three orthogonal reaction wheels, and three orthogonal magnetic torque rods. The ACS has been characterized in flight testing and has demonstrated RMS pointing errors typically below 0.02 degrees for tracking a ground-station location. The spacecraft also incorporate GPS receivers that can be used to develop high-precision orbit ephemeris information. The spacecraft and lasers are further described by Rose[1]. These two spacecraft were launched on November 13, 2017 and deployed from Cygnus OA-8E on December 6, 2017 into an orbit with a nominal altitude of 450 km and an inclination of 51.6 degrees.

The R3 spacecraft (also known as AeroCube-11B, or AC-11) is a 3U imaging-technology demonstrator with a primary mission of exploring pushbroom imaging in a CubeSat. The R3 spacecraft bus is closely based on the design of the OCSD bus, with mostly identical avionics. The ACS incorporates the same suite of sensors and rate gyros, but uses larger reaction wheels and magnetic torque rods to compensate for the greater moments of inertia in the 3U bus. While OCSD was a laser downlink technology demonstrator, the R3 satellite, which launched on December 15, 2018, incorporates a laser transmitter as an operational data downlink channel. The laser is functionally identical to the lasers in the two OCSD spacecraft but incorporates some structural changes required for integration into a slightly different bus. Like OCSD, the R3 laser is body mounted and beam pointing is controlled by the spacecraft ACS. The beam divergence in the R3 laser is 0.10 degrees. This spacecraft is described in more detail by Pack[2].

The ISARA spacecraft is a 3U communications technology demonstrator that had as its primary mission a test and demonstration of a deployable high-gain Ka-band antenna. The satellite also carried an auxiliary

payload, the CubeSat Multispectral Observation System (CUMULOS), which consists of three co-boresighted cameras, one operating in the visible spectrum, one in the short-wave infrared (SWIR) and one in the long-wave infrared (LWIR). Neither the visible camera nor the LWIR camera has sensitivity to the OCSD laser wavelength, but the SWIR camera is sensitive to the 1064-nm wavelength of the OCSD lasers. The ISARA bus is essentially identical to the R3 bus, including all the ACS components, However the ISARA bus does not have a communications laser on board, and data download is via a 915-MHz UHF radio. The CUMULOS SWIR camera is a FLIR Tau SWIR 25 equipped with a vented lens from Stingray Optics. The sensor is a FLIR InGaAs array with 640 by 512 pixels, and is sensitive over the spectral range from 900 to 1700 nm, which includes the 1064-nm wavelength of the OCSD and R3 lasers. The ISARA spacecraft and CUMULOS payload are described in more detail by Hodges[3] and Pack[2,4].

Orbital Dynamics

The two OCSD spacecraft and the ISARA spacecraft were all deployed from the same launch vehicle on December 6, 2017 and started out in nearly identical orbits. Since then, the two OCSD spacecraft, which have nearly identical ballistic coefficients, have been conducting proximity operations experiments using a combination of variable drag and an experimental propulsion system[5] and so remain very close together in orbit. ISARA, on the other hand, does not have a propulsion system, and has a ballistic coefficient substantially smaller than that of the OCSD spacecraft, so has experienced more orbital decay. As a result, by the time these experiments started, a little over a year after deployment, the orbit of ISARA was a few km lower than that of OCSD. Consequently, the orbital period of ISARA was a few seconds shorter than OCSD, and ISARA, although in the same orbital plane as OCSD, would lap OCSD about every two months. For most of the time, ISARA is below the horizon relative to OCSD, but approximately every two months, for a period of several days, the three spacecraft were in range of one another.

The R3 spacecraft, which was launched a year later than the other three, is orbiting at about 500 km altitude and 85 degrees inclination. This orbit brings it within range of ISARA in a series of passes in sequential orbits in a pattern that repeats about every 4.5 days. Figure 1 shows representative plots of the ranges between the various satellites as a function of time.

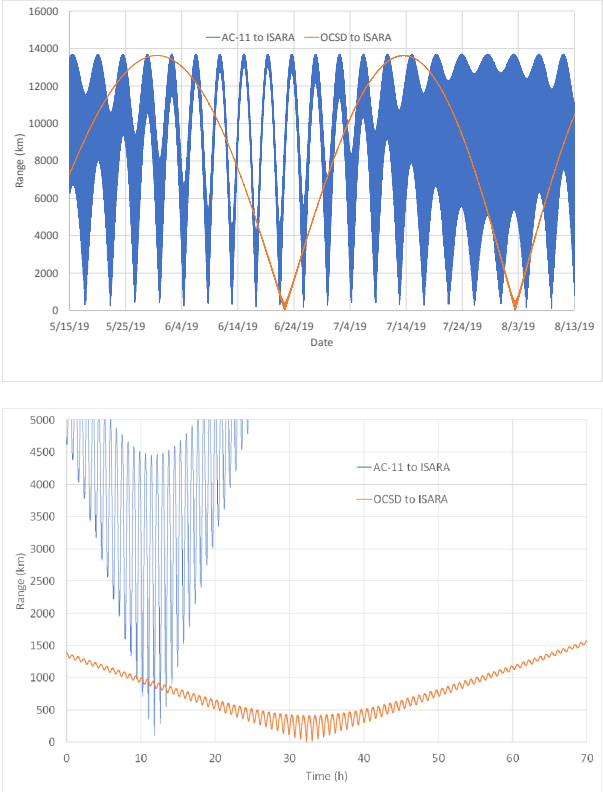

Figure 1. Range between AeroCube-7 and ISARA, and between AeroCube-11 and ISARA. The range variation is shown over a three-month period (top) and a three-day period (bottom).

Before beginning the experiments, we evaluated the minimum and maximum ranges over which the crosslink was possible. The maximum range would be limited either by the minimum signal strength detectable in the SWIR camera, or by the shape of the orbits causing the beam path to intersect the Earth's limb. The minimum range would be limited either by the uncertainty in orbit determination (recall that the beam spot size is smaller at shorter ranges, but the orbit uncertainty is independent of range), or by the potential for the laser beam to damage the camera at the high beam flux possible at very short ranges.

The minimum signal strength detectable by the SWIR camera depends on camera settings and is difficult to define clearly. Thus, we chose to approach it by comparing the expected signal strength at maximum possible range as limited by orbital dynamics to the signal strength clearly observed in existing starfield images acquired by the SWIR camera. The star Alpha Tau (Aldebaran), which was clearly visible in previous images acquired by this SWIR, has a spectral energy distribution that was modeled according to the method of Rudy[6]. For this analysis, we integrated this spectral energy distribution over the spectral range of the SWIR

camera, yielding a total flux of about 14 nanowatts per square meter in Earth orbit.

For two satellites in circular orbits at 450 km altitude, and assuming a spherical Earth for simplicity, the straight-line beam path between them would be tangent to the surface when they are separated by about 4875 km. At greater separations the beam path would intersect the surface, so this number represents the maximum link distance in principle. In practice, however, it would be very challenging to see the laser at this range because of atmospheric distortions, as well as infrared background visible from the Earth's surface and atmosphere. A practical lower limit for the altitude at which the beam can skim the atmosphere is the infrared airglow layer visible in the SWIR camera when viewing the Earth's limb. This layer typically falls between 90 and 100 km altitude. Selecting 100 km as the minimum tangent altitude gives a maximum range of about 4310 km between the two satellites. For the case of R3, where the receiver is at 450 km and the transmitter at 500 km, the maximum range goes up to about 4460 km. At shorter ranges, the laser beam will have an apparent elevation angle above the airglow layer that is determined by the separation between the spacecraft. Figure 2 illustrates the relevant geometry.

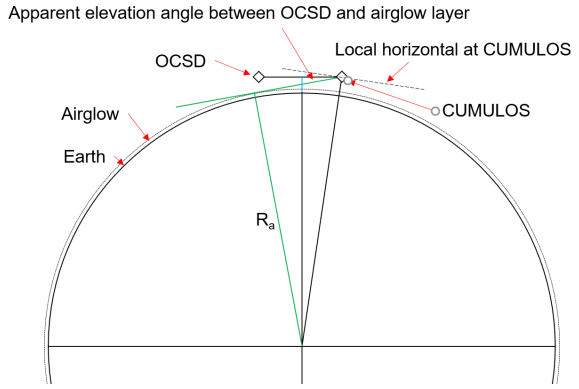

Figure 2. Geometry of an optical crosslink in LEO.

The expected signal strength is a function of range, pointing accuracy, and laser beam properties. The laser beams are profiled in the laboratory prior to launch. For OCSD-B, the beam has a Gaussian profile with a beam divergence of 0.06 degrees FWHM[1], or 0.051 degrees when measured at the $1/e^2$ radius. The centerline beam flux I is a function of distance and is given by $I=2P/\pi w^2$, where P is the total beam power and w is the $1/e^2$ radius of the beam at the range of interest. Figure 3 shows the expected centerline beam flux for the OCSD-B laser as a function of range. At the maximum possible crosslink range of 4310 km, the centerline flux is about 85 nW/m^2, or a factor of six higher than the total IR flux from Alpha Tau. As such, OCSD-B should be clearly visible to the SWIR camera even at the maximum possible crosslink range. OCSD-C has a beam divergence of 0.15 degrees FWHM, so will have a lower centerline beam flux. Nevertheless, even at 4310 km, the OCSD-C centerline flux should be above 13 nW/m^2, and so should be clearly visible to the SWIR camera. The laser in the R3 spacecraft has a beam divergence of 0.10 degrees FWHM, intermediate between the two OCSD lasers, and the expected centerline flux will be about 29 nW/m^2 at the 4460 km maximum range possible between R3 and ISARA.

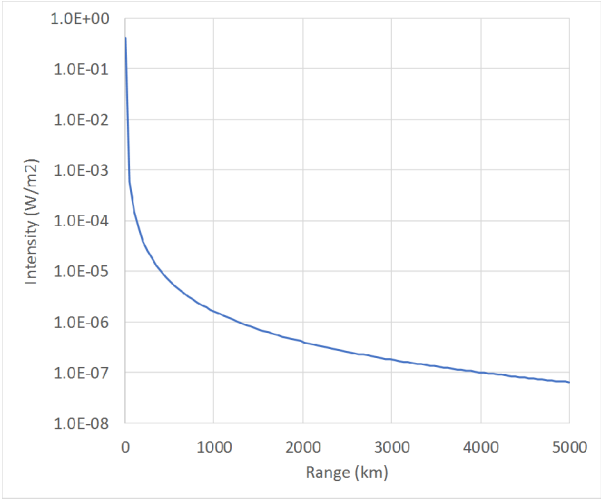

Figure 3. Centerline beam flux as a function of range for the OCSD-B laser.

We also estimated the minimum range at which there is no risk of damage to the SWIR (in operation) or to either of the other two cameras (which would be exposed to the beam, although not in operation). For OCSD-B, which has the highest centerline beam flux, this range was well under 1 km, so would not be a limitation on the experiment.

EXPERIMENTAL PROCEDURE

Conceptually the experiment is very simple; one of the transmitting satellites points its laser toward the ISARA spacecraft while the CUMULOS cameras on ISARA are pointed at the transmitting spacecraft and the SWIR camera acquires images. In practice, there are a few steps along the way.

The first step is to identify opportunities. This involves looking ahead at the forecast orbital positions of the satellites and considering not only range but also other constraints including that the crosslink operations work best if both satellites are in eclipse. Since this is a mission of opportunity, the crosslink operations are also constrained by the priority of other satellite operations.

Once an opportunity has been identified, the satellites will collect GPS fixes for at least two orbits within 24 hours in advance of the experiment to obtain precision ephemeris information. The satellite position information available from published ephemeris data (TLEs) carries an uncertainty of a few thousand meters, which is large compared to the laser spot size at shorter ranges. With the on-board GPS data, the position uncertainty of the satellites can be reduced to a few meters, which is well below the laser spot size, even at ranges as short as 50 km.

The precision ephemeris is used to develop a detailed pointing plan for both spacecraft as a function of time. This is necessary because both spacecraft are pointing open-loop - there is no mechanism for either spacecraft to track the other in real time, so they operate independently, with pointing based solely on the expected positions of both spacecraft. The pointing plan is translated into a set of command sequences, including not only pointing but activation of both the laser and camera. The command sequences are then uploaded to both spacecraft in advance of the expected opportunity. After the scheduled event, as the spacecraft pass over ground stations, the telemetry and images are downloaded for analysis.

RESULTS

The first successful run of the experiment took place on January 9 2019 when the ISARA and OCSD-B spacecraft were over the western Indian Ocean (see figure 4), separated by a range of 1995 km. The direction of motion in figure 4 is from southwest to northeast, and ISARA is leading OCSD-B, so the images are looking back approximately along the orbital track.

During this run, the attitude control system of the OCSD-B spacecraft was commanded to track the ISARA spacecraft, with the laser operating at a constant output. The CUMULOS payload was pointed at the OCSD-B spacecraft and a series of eleven images were acquired at intervals of approximately 3 seconds. During this run, the camera exposure settings were adjusted between frames through a series of steps with the goal of determining optimum camera settings for future runs. Figure 5 shows the first image of this series. One challenge with using a COTS SWIR camera is that this type of camera is known to be susceptible to radiation-induced hot pixels in LEO. This is clearly evident in figure 5; almost all of the bright points seen in this figure are hot pixels. Since hot pixels tend to be isolated single pixels (surrounded by black pixels), the two obviously brighter points of light, which spread across multiple pixels, can be identified as a star and as the OCSD-B laser.

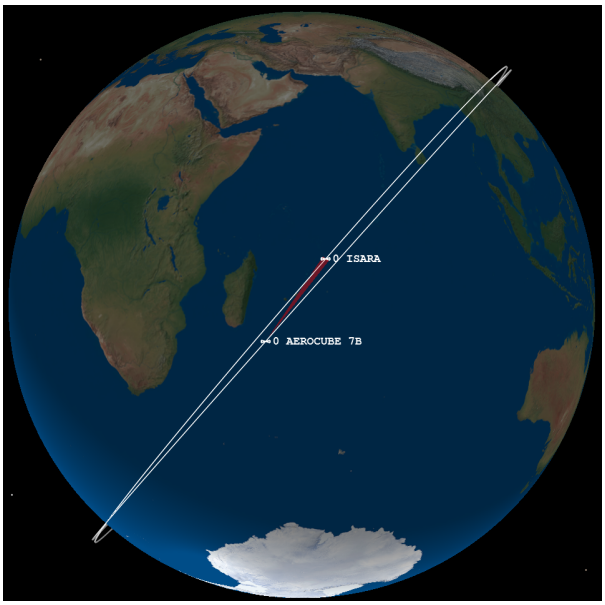

Figure 4. Orbital geometry for the first crosslink experiment.

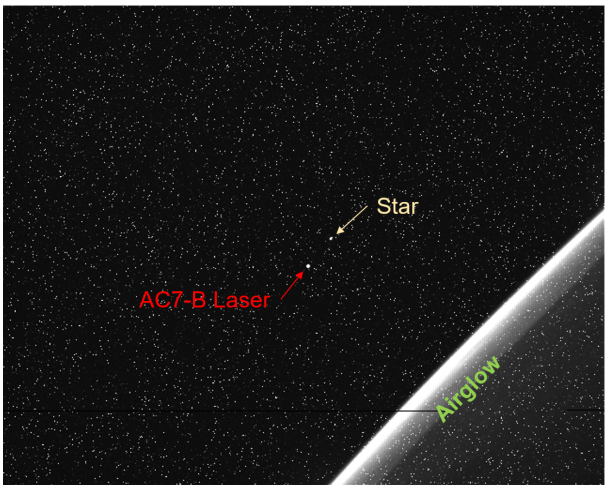

Figure 5. Single SWIR image from first crosslink experiment.

The camera point of view is tracking the OCSD laser as the two spacecraft orbit the Earth, so the position of the laser will not change over successive images, while the apparent position of any stars will. This is evident in figure 6 which shows the result of averaging all eleven images and then subtracting one image to remove most of the hot pixels (which change little from frame to frame). The two stars in the field of view appear to move toward the Earth's limb in successive images due to orbital motion. They also appear to change in brightness due to changes in camera settings. The Earth's limb, on the other hand, does not appear to

move between successive frames because the orbits are approximately circular and the perspective relative to the Earth does not change from frame to frame (see figure 2).

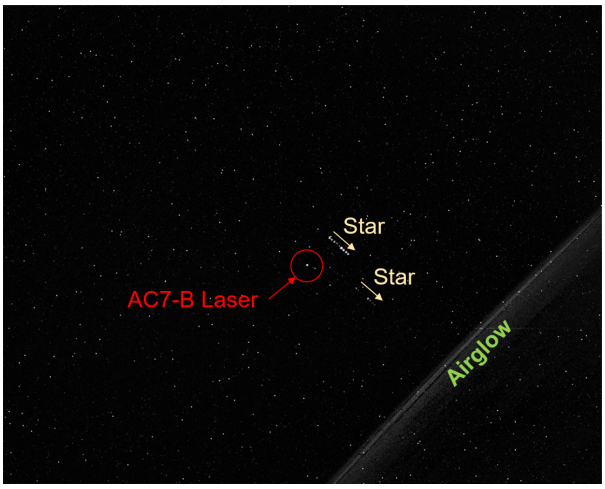

Figure 6. Ten sequential images combined with background subtraction.

Further image processing makes it possible to remove nearly all hot pixels. Figure 7 shows the results of combining two successive images by enhancing the contrast, increasing the brightness, and subtracting the second image from the first. The result of this is several pairs of bright and dark spots with a constant offset corresponding to orbital motion, where the bright spots are stars seen in the first image and the dark spots are locations of the same stars in the second image. This approach makes it possible to unambiguously determine the locations of a moderate number of stars in the image which, when compared to an infrared sky map, are easily identified, as indicated in figure 7. The difference between the infrared sky and the visible sky is brought out by the presence in this image of some rather obscure stars along with the absence of some stars that are fairly bright in the visible sky. For example, the star Alnair (Alpha Gruis), which has a visible magnitude of 1.7 can be found in the image only by reference to nearby stars. In contrast, the nearby star Pi Gruis, which has a visible magnitude that varies between 5.3 and 7, is clearly identifiable in the image.

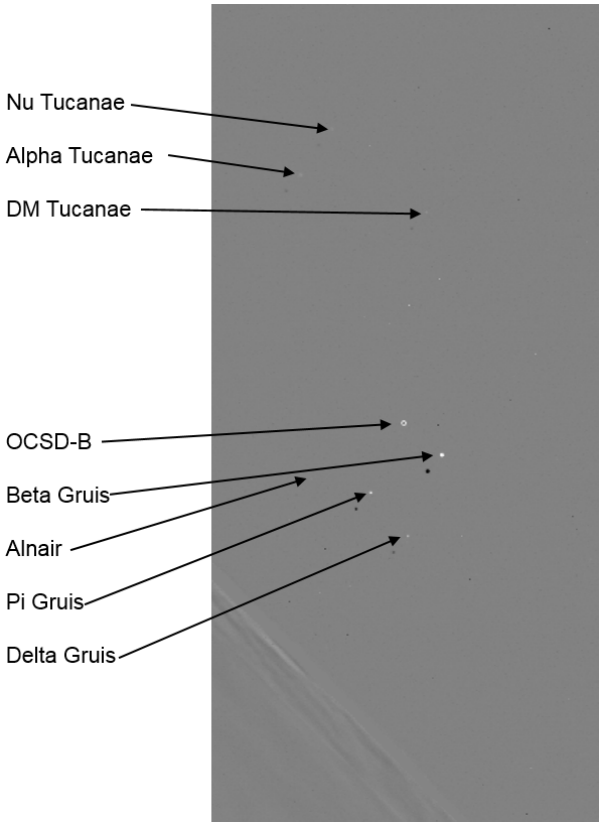

Figure 7. Subtracted image pair after contrast enhancement and hot pixel removal.

The second experimental run with OCSD-B occurred on 15 March 2019, with the two satellites over the western Pacific Ocean, separated by a distance of 2292 km. Again, ISARA is in the lead, looking back along the orbital track to OCSD in a generally southwesterly direction. This experiment was intended as a pathfinder for beam-profile measurements. As with the previous test, ISARA was programmed to have the CUMULOS payload track the location of the OCSD spacecraft and acquire images. In this case, the SWIR images were acquired at ten-second intervals with constant camera settings. While the images were being acquired, the OCSD spacecraft was programmed to slowly sweep the laser beam across the location of the ISARA spacecraft. The intention was to measure beam intensity at the camera as a function of time by evaluating the images, then correlate the signal strength with the laser pointing to estimate beam profile. The experiment was qualitatively successful in that the beam could be clearly seen increasing and decreasing in intensity as it swept across the camera. However, the camera exposures were too long and the laser saturated the pixels in most of the exposures, making a quantitative measurements of signal strength impossible. In addition, the camera frame rate was too slow compared

to the slew rate of the laser, leaving only five images in which the laser was visible.

Figure 8 shows an image of the OCSD laser as well as one star acquired in the second run. Although the field of view included the star Canopus, the brightest visible star in the southern hemisphere, a careful review of the orbital ephemeris data indicated that the star visible in the image is actually R Doradus, which is the brightest infrared star in the southern hemisphere but has a visible magnitude that varies between 4.8 and 6.6. Canopus, which has a visible magnitude of -0.7 but is not nearly as bright in the IR, is also very faintly visible near the top of the frame. Because of the brightness of the OCSD laser, the required SWIR camera exposures are very short and only a few of the brightest IR stars can be seen. In the two successful runs to date we were fortunate to have stars clearly visible in the frame - in much of the sky there are no IR stars bright enough to be seen at the camera settings used to acquire the images of the OCSD-B laser.

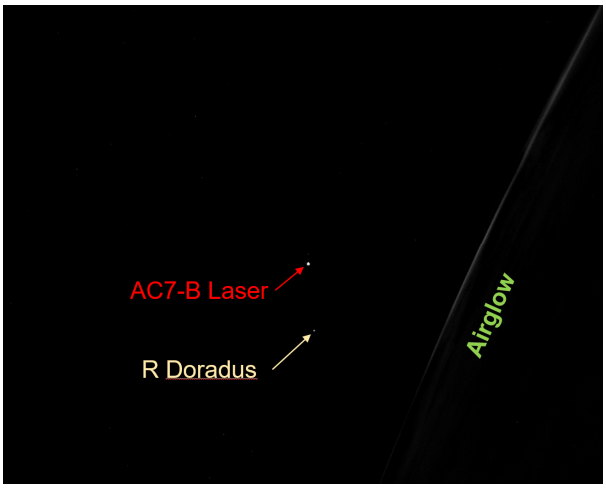

Figure 8. Image of OCSD-B laser and R Doradus from second experimental run.

One additional positive result that came out of the second experiment run was the observation that the image of the OCSD laser was centered on the same SWIR camera pixel as in the first run. This indicates that ISARA is capable of tracking the OCSD spacecraft with a precision at least comparable to the single-pixel field of view of the SWIR camera, which is about 0.1 degrees.

FUTURE WORK

Two experimental runs were conducted with AC-11 as the transmitter. This is a somewhat more challenging test since AC-11 is in an orbit inclined about 25 degrees relative to the orbit of ISARA, meaning that there will be significant relative motion between the satellites and they will have to slew to keep the laser beam and cameras aligned with one another. In both runs, however, no image data was acquired. Telemetry indicated that AC-11 performed the programmed attitude maneuvers and turned on the laser. However, the command sequence on ISARA failed to initialize for reasons that are still being evaluated. As of this writing, further attempts at crosslink pointing using AC-11 and ISARA are planned.

Three additional improvements are also planned for the beam-profile measurements. First, additional experiments will be used to refine the camera exposure settings to ensure that we do not saturate the pixels at peak exposure. Second, a code modification to the ISARA SWIR camera controller will allow sub-framing. The results to date indicate that ISARA can point well enough that we do not need a full frame to ensure that the laser is captured by the camera. Since the downlink bandwidth on ISARA is very limited, the reduction of the frame size by one to two orders of magnitude will allow us to acquire ten to 100 times more frames. Third, we will adjust the OCSD slew rate and the SWIR camera frame rate to ensure that we get far more than five exposures as the beam sweeps across the camera. The increase in the number of images as the intensity ramps up and down will give a much higher spatial resolution on the laser beam profile measurement.

CONCLUSIONS

The goal of this mission of opportunity was a practical demonstration that one CubeSat in orbit can track another with sufficient precision to achieve an optical crosslink. Although no data was transferred (nor was there any intention to pass data), the exercise demonstrated that crosslink pointing and tracking is possible. Further, a pathfinder test indicates that optical crosslinking has the potential to provide a means for on-orbit optical beam profile measurements that will be free of atmospheric distortions. Future tests are intended to demonstrate optical crosslink pointing with more challenging orbital dynamics, and to obtain quantitative beam profile measurements.

Acknowledgments

This work was supported by The Aerospace Corporation's Internal Research and Development funding. The R3 spacecraft was supported by The Aerospace Corporation's Internal Research and Development funding. The OCSD and ISARA missions were supported by NASA's Small Spacecraft Technology Program (SSTP).

REFERENCES

1. 1. T.S. Rose, D.W. Rowen, S. LaLumondiere, N.I. Werner, R. Linares, A. Faler, J. Wicker, C.M. Coffman, G.A. Maul, D.H. Chien, A. Utter, R.P. Welle, and S.W. Janson, "Optical Communications Downlink from a 1.5U CubeSat: OCSD Program," SmallSat 2018, SSC18-XI-10
2. 2. Dee W. Pack, David R. Ardila, Eric Herman, Darren W. Rowen, Richard P. Welle, Sloane J. Wiktorowicz, and Bonnie W. Hattersley, "Two Aerospace Corporation CubeSat Remote Sensing Imagers: CUMULOS and R3," SmallSat 2017, SSC17-III-05.
3. 3. Richard E. Hodges, Dorothy K. Lewis, Matthew J. Radway, Armen S. Toorian, Fernando H. Aguirre, Daniel J. Hoppe, Biren N. Shah, Andrew A. Gray, Darren W. Rowen, Richard P. Welle, Andrew E. Kalman, Adam W. Reif, and Jerami M. Martin, "The ISARA Mission – Flight Demonstration of a High Gain Ka-Band Antenna for 100Mbps Telecom," SmallSat 2018, SSC18-VI-03.
4. 4. Dee W. Pack, Christopher M. Coffman, and John R. Santiago, "A Year in Space for the CUbesat MULtispectral Observing System: CUMULOS," SmallSat 2019, SSC19-XI-01
5. 5. Darren Rowen, Siegfried Janson, Chris Coffman, Richard Welle, David Hinkley, Brian Hardy, and Joseph Gangestad, "The NASA Optical Communications and Sensor Demonstration Program: Proximity Operations," SmallSat 2018, SSC18-I-05
6. 6. R.J. Rudy, "Models of Stellar Spectral Energy Distributions for the Optical and Infrared," Aerospace Technical Report ATR-2007(8189)-1, 25 January 2007.

.